



**Michigan
Technological
University**

Michigan Technological University
Digital Commons @ Michigan Tech

Dissertations, Master's Theses and Master's Reports

2023

EVALUATING GEOMECHANICAL UNCERTAINTY IN OPEN PIT MINE PLANNING

Evan Ricchio-Hitchcock
Michigan Technological University, ejricchi@mtu.edu

Copyright 2023 Evan Ricchio-Hitchcock

Recommended Citation

Ricchio-Hitchcock, Evan, "EVALUATING GEOMECHANICAL UNCERTAINTY IN OPEN PIT MINE PLANNING",
Open Access Master's Thesis, Michigan Technological University, 2023.
<https://doi.org/10.37099/mtu.dc.etr/1573>

Follow this and additional works at: <https://digitalcommons.mtu.edu/etr>



Part of the [Geological Engineering Commons](#)

EVALUATING GEOMECHANICAL UNCERTAINTY IN OPEN PIT MINE
PLANNING

By

Evan Ricchio-Hitchcock

A THESIS

Submitted in partial fulfillment of the requirements for the degree of

MASTER OF SCIENCE

In Geological Engineering

MICHIGAN TECHNOLOGICAL UNIVERSITY

2023

© 2023 Evan Ricchio-Hitchcock

This thesis has been approved in partial fulfillment of the requirements for the Degree of MASTER OF SCIENCE in Geological Engineering.

Department of Geological and Mining Engineering Sciences

Thesis Advisor: *Dr. Snehamoy Chatterjee*

Committee Member: *Dr. Luke Bowman*

Committee Member: *Dr. Mohammadhossein Sadeghiamirshahidi*

Department Chair: *Dr. Aleksey Smirnov*

Table of Contents

Acknowledgements.....	4
Abstract.....	5
1 Introduction.....	6
2 Materials & Methods.....	9
2.1 Materials.....	9
2.2 Methods.....	10
2.2.1 Geological Modeling & Resource Estimation.....	10
2.2.2 RQD Modeling and Slope Stability Analysis.....	12
2.2.3 Open Pit Optimization.....	16
3 Results & Discussion.....	18
3.1 Exploration Drilling & Statistics of Gold Grades.....	18
3.2 Geological Modeling.....	20
3.3 RQD Percentages of Each Rock Type.....	25
3.4 Slope Stability.....	29
3.5 Pit Optimization.....	32
4 Conclusion.....	35
4.1 Limitations and Further Studies.....	35
5 References.....	36

Acknowledgements

I would like to thank my advisor, Dr. Chatterjee, my committee, my family, and my friends for the tremendous amount of support they gave me while furthering my education.

Abstract

Open pit mine planning encompasses a variety of uncertainties. Uncertainty due to geomechanics is most critical for a safe operation in an open pit mine. Without sufficient knowledge of the geomechanical properties of the subsurface, a reliability analysis of the slope stability could be challenging. Slope stability is a crucial step in pit optimization since the cash flow analysis of a mine is constrained by a stable slope angle. However, obtaining a stable slope angle with certainty is difficult to achieve as geomechanical parameters are modeled using a very limited number of samples. This thesis proposes a method to integrate geomechanical uncertainty, specifically uncertainty regarding slope stability, in pit optimization through reliability-based analysis. This research explores gold deposit data received from exploration drilling in Alaska, with potential to build an open pit mine. The gold grade was estimated by ordinary kriging (OK) using exploration drilling data. Rock Quality Designation (RQD) is the only geomechanical data available from this deposit, and it was used to calculate cohesion, angle of internal friction, and unit weights of the rock. The uncertainty of the RQD was quantified for each rock type of the deposit. The probability density function (PDF) of RQD for each rock type was fitted using log-normal distribution. The uncertainty-based slope stability analysis was carried out using the limit equilibrium method. The reliability and failure probability of the different slope angles were calculated, and the maximum slope angle with 100% reliability is 50° . The cash flow for each slope angle was identified and assessed along with the probability of failure for three different factor of safety values. The results showed that the steeper the slope angle used, the more profit would be generated, but the probability of failure increased. In contrast, using shallower slopes did not generate as much profit, but the probability of failure was lower. A threshold slope angle of 51.5° was determined to be the highest angle that can be utilized without the probability of failure outweighing the profit generated.

1. Introduction

In any structural or slope stability analysis of an open pit mine, geomechanical properties of rock masses must be understood thoroughly. Ignoring the importance of these properties can lead to significant losses in terms of personnel, equipment, safety, time, production, and capital (Zebarjadi Dana et al., 2018). When these properties are understood, the likelihood of slope failure decreases and ensures the workers and equipment are safe during mining operations. Not only do the knowledge of these properties help ensure safe working conditions, but they play critical roles in determining the optimum slope angle in the mine. The smallest changes to the overall slope angle for an open pit mining operation can influence the economic value of the mine significantly (Ning et al., 2011). The challenge that is faced in many open pit mining operations, however, is how to maximize profit while maintaining stability of the slopes throughout the mine. If a steeper slope angle is used, the lower the stripping ratio will be which will result in a more profitable mining operation (Mitma, 2020). However, if a steeper slope angle is used, this decreases the slope stability which increases the risk of slope failure in the mine. The ideal mining operation will want to maximize profit while preserving the slope stability and safety of the mine.

Slope stability is indexed by a measurement known as the Factor of Safety (FoS). Also referred to as the Safety Factor, is a measure used in engineering design to represent how much greater the resisting capacity of a structure or component is relative to an assumed load. With respect to slope stability, FoS is the ratio of shear resistance to driving force along a potential failure plane. There are multiple methods available to calculate the factor of safety for slope stability analysis, such as the limit equilibrium method (Huang, 2014), finite element method (Liu et al., 2015), finite difference method (Soren et al., 2014), and discrete element method (Lu et al., 2018; Zebarjadi Dana et al., 2018). A factor of safety greater than 1.0 implies the slope is stable; if FoS is equal to one, the slope is at the verge of failure; and if the FoS is less than one, the slope is unstable (West et al., 2018). FoS of a slope is an estimate based on standard industrial methods with inferred material parameters from laboratory or drilling data sources under different loading conditions. To calculate FoS of a slope, the equation below is used:

$$\text{Factor of Safety} = \text{Shear Strength} / \text{Shear Stress} \quad (1)$$

Hypothetically, for any subsurface description to determine soil or rock mass behavior should encompass all properties in the subsurface body including all spatial variations of the given properties. This is not possible since one would need to depict the

rock and/or soil mass and describe/test every inch of the ground material (Hack et al., 2006). That is why exploration efforts are critical in the beginning stage of open pit mine planning. Exploration methods encompass geological, geochemical, geophysical surveys, drill holes, trial pits, and underground openings. Detailed sampling such as drill cores, are generally spaced relatively close to one another to ensure the geological subsurface is defined properly (Hustrulid et al., 2013). However, drill hole data is usually limited for a mining project, which in turn could yield a variety of possible outcomes for an orebody (Menabde, 2018). Due to drillhole limitations, geomechanical and mining engineers use different geotechnical parameters to create a prospective model of the open pit mine. Generally, a deterministic boundary model is created to divide the mine site into multiple geomechanical domains based on the available data at the prospective mine site. Each geomechanical domain is assigned a geomechanical property value by averaging all the data falling within that domain, which is then used to determine slope stability for an open pit mine (Hack et al., 2006; Read et al., 2009). Since this model uses an average geomechanical property value, this infers the rock masses to be homogeneous, which does not differentiate the rock properties as they would be in the field. Some rock masses might have structural impurities such as mineral veins that change the strength of the rock body in the area, or dikes that are of different lithology unaccounted for (Kring et al., 2020).

In addition to the lack of data in all locations of a prospective mine, the assumption of a homogenous rock mass invites geomechanical uncertainty into the design of an open pit model. With geomechanical uncertainty in the design of open pit mines, it can be difficult to assess whether a model is safe and how to assess the economic benefits that would come from the mine. It is not possible to make a safe decision based on a single deterministic analysis by itself unless the ground profile, soil behavior, physics, and construction effects are known, can be computed to perfect accuracy, and there are no unknown variables (Phoon et al., 2022). Geomechanical uncertainty also stems from the historical background of the prospective area. Since the subsurface of the Earth was formed under a broad variety of complex physical conditions and no one was able to observe it, there is a knowledge gap in regards to the history of an area; hence why geomechanics encompasses large uncertainties (Curran et al., 2006). Previous studies have quantified geomechanical uncertainties and evaluated their impacts on slope stability. For example, Kring and Chatterjees (2020) applied two geostatistical simulation algorithms to quantify spatial uncertainty of Rock Quality Designation (RQD) values and fault zones. The resulting values were applied in a slope stability analysis which yielded reliability of different slope angles of an open pit gold mine. Another study on Sungun Copper Mine in Iran used three methods to quantify uncertainty within the slope stability analysis: Taylor series, Rosenblueth point estimate, and Monte-Carlo simulation method. The results showed that the Monte-Carlo simulations proved best and

most effective regarding precision reliability for slope stability analysis (Abbaszadeh et al., 2011). When it comes to review of methods for slope stability analysis, it's shown that the deterministic approach tries to provide a reliable analysis with slope design recommendations, but fails to illustrate slope safety performance, which gives critical information on the factor of safety and risk of failure (Abdulai et al., 2019). Another study quantifying geomechanical uncertainty, conducted by Abdulai et al., (2021), demonstrated the use of probabilistic based analyses and compared it with a deterministic stability analysis on slope design with an open pit mine in Western Australia. He found that verification from deterministic finite element methodology in RS2 (Rocscience RS2, Version 11.007) is needed but the overall probabilistic analysis of slope designs yielded better results in quantifying uncertainty on slope design. A case study located on an open pit mine in the Andean region of Peru, analyzed the validity of existing bench slopes by kinematic and kinetic analyses with both deterministic and probabilistic approaches. The results showed that the probabilistic approach was favored not only due to quantitatively being able to measure critically occurring discontinuities due to variability in orientation, but also provides the engineers with more power to assess, review or validate bench slope design performance (Obregon et al., 2019).

The studies mentioned analyze slope stability in a variety of ways, but do not use the resulting slope stability analysis in pit optimization. As previously mentioned, the ideal mining operation will want to maximize profit while preserving the slope stability and safety of the mine. To maximize profit, open pit mine optimization must be conducted to see if the mining operation can maximize its economic value (Paithankar et al., 2021). Open pit optimization algorithms are used to determine the scope of deposit development required to ensure profitability while meeting the requirements for mine development. Incorporating uncertainty from technical, geological, and mining sources such as variability of the orebody grade, and quality of ore, should be acknowledged due to the importance of these variables (Dimitrakopoulos et al., 2004). General approaches for mine optimization are typically based on a single estimation model for the orebody but does not acknowledge the in-situ variability and uncertainty related with the orebody description. Conditional simulations based on drill hole data are able to generate several scenarios of a deposit, showing in-situ variability of spatial continuity which addresses the shortcomings of estimation methods. However, this can be inimical if the in-situ grade variability is ignored and the uncertainty in the orebody is documented, by decreasing the net present value from what was forecasted (Benndorf et al., 2012). Mine optimization algorithm utilizes Block Economic Value (BEV), which calculates the profit from a block that is used as input data for the algorithm. Block Economic Value represents the revenue estimated by dividing the 3D orebody model created off geological data into blocks, and then considering sales revenue and production cost for each block. However, the end results of open pit optimization algorithms that utilize BEV

as input data also contain uncertainty. Uncertainty using this method for mine optimization are due to the variation in mineral prices. Multiple variables such as production costs, exchange rates, and taxes are also not considered in open pit mine optimization but could be applicable with the same method used to calculate the mineral prices (Baek et al., 2016). Other research that explores open pit optimization such as the case study conducted by Paithankar et al. (2021) focuses only on the supply uncertainty and uncertainty in regard to the economic value in open pit mining complex optimization but does not consider mining width constraints. It should be noted that although these past studies look at pit optimization and include uncertainty of different kinds, implementation of geomechanical uncertainty is not evaluated in them.

This paper proposes the utilization of open pit optimization under geomechanical uncertainty, more precisely uncertainty of slope stability of an open pit mine. This proposed research directly utilizes geomechanical uncertainty, stemming from exploration drilling, to obtain a constant FoS used at an open pit mining operation that will ensure the safety of the mine while preserving the greatest possible profit generated. This integration of geomechanical uncertainty in open pit optimization will not only provide a viable interpretation of slope stability, but also will assess the economics each slope angle yields for the given open pit mine. With this information, mining operations can decide what would be the most beneficial slope angle that can generate the maximum amount of cash flow while ensuring the mine is operating safely.

2. Materials & Methods

2.1 Materials

The data involved in this study includes 145 core drill holes with RQD, lithology, and assay grade from a gold exploration project in the interior region of Alaska. The total collected depth of the drillholes was 140,854 ft (42,932 m), with a calculated average depth of 261 meters per drillhole. The core samples were collected at a spacing of 75 m inclined at around -50° . The site is being inspected for a potential open pit mine operation. The study area was used for reference regarding the geological and geomechanical background for this research. The gold is mainly located in quartz veins associated with intrusive dikes. A complex geological package engulfs the deposit with interleaved sedimentary and volcanic rocks. The rocks in this area have experienced major deformation events such as: folding, thrusting, dike intrusions, and collapse of rock. Due to these events, there are heavily fractured, weak to moderate strength rocks in the area. There was a total of nine different rock bodies identified within the project area, but five of the nine rock bodies were excluded from the study. This was due to the size

and recurrence of the five rock bodies in the subsurface, along with providing no benefit to gold grade estimations. Along with providing no benefit to gold grade estimations, the excluded rock types are located near the surface, so pre-stripping activities would remove these rock bodies and ultimately provide zero benefit to the slope stability analysis. However, the four main rock types utilized in this study go as follows: Cambrian (CAM), Upper Sediments (UPS), Main Volcanics (MVC), and Lower Sediments (LOS). Depending on the location of sampling, MVC comes in contact with both the CAM and LOS which is a result of the heavily faulted area. Although the assay grades are available for almost all drill holes, the geomechanical parameter (only RQD) is available for 27 drill holes, with no other strength parameters given.

2.2 Methods

The proposed research’s methodology is split into four sections (1) geological modeling and grade estimation; (2) geomechanical parameters simulation; (3) uncertainty-based factor of safety calculations & slope stability analysis; and (4) open pit optimization under geomechanical uncertainty. Figure 1 demonstrates the steps of this research.

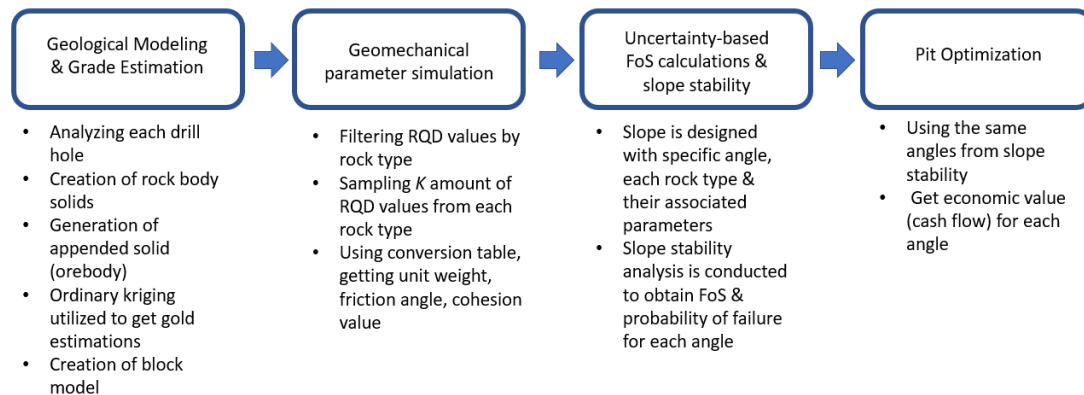


Figure 1: A flow chart illustrating how this research was conducted, with brief explanations of each step.

2.2.1 Geological Modeling & Grade Estimation

The first step was to analyze the exploration drill hole data. This was done by looking at each drill hole, and seeing what rock types were present. For solid model

preparation, the North-South section lines were drawn with 100 m interval. In each section, all four rock-types were digitized. This allowed to see the extent of each rock type present, and how they were structurally layered. When complete, valid solid was generated for each rock type, they could be appended together to create a complex solid. A valid solid indicates there are no discrepancies within the solid, such as over lapping polygons or openings within the solid and ensures further analysis can be conducted using the solid. With a complex solid, this enabled an illustration of the subsurface to be made, which then provided an orebody to use for mineral resource and geomechanical parameter estimation.

The main goal with resource estimation is to generate a block model that contains estimated gold grade. The grade estimation was based off the gold grades found in the exploration drilling data. Before resource modeling, the gold assay data was composited to make a unique sample length. For this research composite length of 1 m was selected to minimize the dilution and generate enough composite samples (Kapageridis et al., 2013). However, the geology had to be preserved while compositing to see the gold grades in each rock type. This was done by using an “assay” file to create a rock code based off the lithology, and projecting over the “Z” plane. Missing data had default values assigned to them, which then were filtered out to ensure proper gold grades were assessed. Once compositing was done while preserving the geology, resource estimation could be conducted.

Before resource modeling, spatial continuity modeling was performed. Experimental variogram was calculated using the composited samples. The directional anisotropy was tested by calculating a Rose Diagram (Ecker et al., 1999). The best fitted theoretical function was fitted before resource estimation, and a spherical structure had to be created and best fitted for the ore deposit. The type of estimation used was block model estimation and the estimator used was ordinary kriging (OK). OK was decided on since this kriging method is widely used to estimate a value at a point of a region for which a variogram is known. It uses data that is in the general area of the estimation location, and it can also be used to estimate a block value (Wackernagel, 2003). However, discretization was conducted to get block grades. Discretization is the process to subdivide space into a series of points or the method used for transforming a coarse grid into a set of conforming fine grids (Sunday et al., 2020). The discretization steps were as follows: 4 steps along the X direction, 4 steps along the Y direction, and 4 steps along the Z direction. By doing discretization, we are creating 64 (4x4x4) points within a 5x5x5 meter block. These 64 points were used to calculate the block grades as mentioned previously. Once OK was conducted, a block model was created with a topographical surface applied to cut off any gold grade values that were above the surface, decreasing the total number of samples. This resulted in having an estimation of the gold ore deposit within each rock type and the overall rock body based off the exploration drilling data.

2.2.2 RQD modeling and Slope Stability Analysis

Rock Quality Designation was used to assess strength parameters since no data regarding the rock types' cohesion or friction angles exists. Previous research shows that the geomechanical parameters of rock for slope stability analysis can be derived from the RQD (Deere et al., 1988; Kring and Chatterjee, 2020). Ideally for RQD modeling, performing spatial interpolation using the drill holes RQD data for each rock type would provide the best results. Unfortunately, a limited number of RQD data are available within each rock type (Table 1). Therefore, generating a spatial continuity map, i.e., variograms are difficult to achieve. In this research, the uncertainty of the RQD was modeled for each rock type by filtering the RQD data through each rock type identified, so that the RQD data was split by rock type. Filtering enabled a histogram to be created for each rock type showing general statistics, including a mean RQD value. With the RQD values from each rock type, Table 2 (Deere et al., 1988) is used as it converts the RQD value into parameters needed for a slope stability analysis; unit weight, cohesion, and friction angle. However, since is a stochastic approach for geomechanical uncertainty, each rock types histogram were evaluated further by taking K amount of RQD values from each rock type and putting it through Table 2. The K amount of RQD values were taken based off their respective rock types histogram distribution. With the assigned RQD values for each rock type and the corresponding strength parameters from Table 2, general statistics were generated to use for a stochastic analysis for slope stability and factor of safety calculations.

Table 1: The number of RQD samples per rock type used in this study.

Rock Type	# of Samples
CAM	702
UPS	3030
MVC	1739
LOS	1666

Table 2: An illustration correlating RQD percentages with unit weight, cohesion, and angle of internal friction (Deere et al., 1988).

<u>RQD Designation</u>	<u>Unit Weight (kN/m³)</u>	<u>Cohesion (kPa)</u>	<u>Angle of Internal Friction (degree)</u>
Very Poor ($0\% \leq \text{RQD} < 25\%$)	20	150	15
Poor ($25\% \leq \text{RQD} < 50\%$)	20	750	20
Fair ($50\% \leq \text{RQD} < 75\%$)	20	2,500	26
Good ($75\% \leq \text{RQD} < 90\%$)	20	10,000	45
Excellent ($90\% \leq \text{RQD} < 100\%$)	20	50,000	63
Fault	20	150	15

Using the converted cohesion and internal friction angles gathered from the RQD values, slope stability analysis is conducted using the limit equilibrium method. This method defines a proposed slip surface and analyzes the surface to gather the factor of safety. Two-dimensional sections are analyzed presuming plane strain conditions. Linear (Mohr-Coulomb) or non-linear relationships are assumed between shear strength and normal stress on the failure surface constituting the shear strengths of the materials along the potential surface plane.

The critical slip surface where the factor of safety is the lowest value is calculated from the functional slope design. Contrasting numerical models use different optimization strategies to pinpoint the failure surface. A common approach to locate the failure surface utilizes heuristic techniques with search optimization. These techniques look at the stability of different layered slopes. Heuristic optimization considers circular and non-circular surfaces, and external forces to the slope, such as side effects from earthquakes or stabilization forces. Softwares for numerical modeling calculations derive in accordance with various methods of slices. The research presented uses the Bishop limit equilibrium method. Three different assumptions are made in regards to this method: (a) the failure occurs by rotation of a mass of the material on a circular slip surface; (b) the forces on the sides of the slice are horizontal; and (c) the total normal force acts at the center of the base of each slice. The Bishop method does not meet all the equilibrium conditions, but FoS that came from this method agree with FoS calculated from finite element methods. The limitations of the Bishop's method are understood, but

F = Factor of safety	$S_m = \frac{c + N \tan \Phi}{F}$	S_m = Mobilized shear strength
W = Weight of slice		U = Pore water pressure
N' = Effective normal force		W_w = Surface water force
μ = Angle of inclination of external load		K_h = Horizontal seismic coefficient
Z_R = Right inter-slice force		Z_L = Left inter-slice force
δ_R = Right inter-slice force inclination angle		H_L = Height of force Z_L
H_R = Height of force Z_R		α = Inclination of slice base
β = Inclination of slice top		b = Width of the slice
h = Average height of slice		h_a = Height to the center of the slice
δ_L = Left inter-slice force inclination angle		

Figure 2: An illustration of how forces act on a typical slice with explanations for each variable.

The ordinary method of slices is the simplest method of slices. This method obtains the factor of safety, presuming the interslice forces are parallel to the base of each slice. Only normal forces are considered, and interslice forces are ignored in the Bishop method. To make this method computationally efficient, trial and error is utilized to get a factor of safety. The Rocscience Slide2 (Rocscience Slide2, Version 9.025) program is used for slope stability analysis. Using the RQD values and their associated parameters, a slope stability analysis is conducted and the factor of safety is calculated. Quantifying the uncertainty regarding slope stability, a factor of safety is calculated for different slope angle.

A N number of random samples from the rock types RQD distribution were used for uncertainty quantification, are used for the factor of safety calculation, and Bishop method pit slope stability. A total number of N factor of safety values can be generated for uncertainty quantification of the pit slope. Each set of geomechanical parameters from four different rock types created had its slope factor of safety calculated and the factor of safety, F 's, mean value (μ_F) calculated by:

$$\mu_F = \frac{1}{N} \sum_{i=1}^N F_i \quad (3)$$

Where F_i is the factor of safety calculated for the i^{th} randomly simulated geomechanical parameters.

Using the central limit theorem, the probability of failure of the proposed slope stability model which implements uncertainty is calculated as:

$$p_F = \frac{n_F}{N} \quad (4)$$

Where $n_F = \sum_{i=1}^N I(F_i)$ and $I(F_i)$ is a function defined as:

$$I(F_i) = \begin{cases} 1 & \text{if } F_i \leq Th \\ 0 & \text{if } F_i > Th \end{cases} \quad (5)$$

Where Th is the threshold value of the factor of safety.

The steps involved for the uncertainty of the slope stability analysis are as follows:

1. Generate histogram of RQD for each rock type.
2. Convert histogram to unit weights, cohesion, and angle of internal friction using Table 2.
3. Generate N number of unit weights, cohesion, and angle of internal friction for each rock type by randomly sampling from the distribution.
4. For $i = 1$ to N
 - a. Assign the unit weights, cohesion, and angle of internal friction to each rock type
 - b. Calculate factor of safety of i^{th} map using Bishop method
 - c. End *for*.
5. Calculate the distribution function of factor of safety and the probability of failure using Eq. (3) and (4).

2.2.3 Open Pit Optimization

The final pit limits of an open pit mine define what is economically mineable from a given deposit. It determines which blocks should be extracted and which ones

should be left in the ground (Dagdelen, 2001). Open pit mining operations depend on the proper design of the ultimate pit for optimal production planning (Chatterjee et al., 2016). The objective of open pit optimization is to determine the economic value of mineable reserves, in which profit will be maximized but also satisfy the slope angle. The maximum flow minimum cut algorithm is used, which solves the problem of finding a maximal closure within a mine graph where a minimum cut determines an optimal pit contour (Hochbaum, 2001). The algorithm utilized solves the issue of finding the best combinations of desirable and undesirable blocks that results in the maximization of profit (Hlajoane, 2020). For a given slope angle, to calculate the ultimate pit optimization, the following equations were used:

Objective Function:

$$\text{Maximize } \sum_{\gamma \in \Gamma} \sum_{b \in B} v_{\gamma b} x_b \quad (6)$$

$$x_b - x_{b'} \leq 0, \quad b' \in \xi_b, b \in B \quad (7)$$

$$x_b \in \{0,1\}, b \in B \quad (8)$$

Where, $v_{\gamma b}$ is the economic value of mining block b from simulation γ . x_b is the binary decision variable, which takes value 1 if mining block b is inside the pit, 0 otherwise, b' is the block that needs to mine before mining block b to satisfy slope constraints, Γ is number simulated orebody models, and B is the number of mining blocks present in the orebody model. The equation in Eq (6) attempts to maximize the total profits from the deposit where the equation right below represents precedence constraints, which ensures respecting the slope of the ultimate pit. Coming from resource estimation, only the measured and indicated resources that are meeting economic and slope constraints within the ultimate pit are categorized as proven and probable reserves (Hlajoane, 2020).

3. Results & Discussion

3.1 - Exploration Drilling & Statistics of Gold Grades

Figure 3 shows drill holes' locations from the deposit along with each rock type identified. One thing to note from Figure 3 is that although it shows nine different rock types, only four were assessed. This is due to the scarcity of the other rock types and how little they were displayed in the drill hole data; it would be difficult to justify including such small rock types in the analysis. The smaller rock types also do not show up in the majority of the drill holes as compared to the four rock types that are categorized. The rock types distribution over all the drill holes stay relatively in the same order from top down; CAM, UPS, MVC, then LOS. Some discrepancies arise in the order of rock types due to faulting in the area. Once the rock types were assessed, basic compositing was conducted to get an understanding of the gold grades (g/mt) present (Figure 4). The gold grades are all relatively low with grades between 0 and 0.050 g/mt with occasional thin slices of higher gold grades. The higher gold grades seem to show up at random and do not have a pattern within the orebody. Table 3 shows the general statistics for the overall gold grades while Table 4 shows the general statistics for gold grades associated with the four rock types used in this analysis. The average grade within all rock types is 0.012 g/mt which is consistent with how low the gold grade is distributed throughout the subsurface. However, when looking at individual rock types, MVC has a higher average grade at 0.020 g/mt, which is expected as the gold deposit is associated with igneous composition. The lowest gold grades recorded are in the LOS. The total number of samples shown in Table 3 to Table 4 decrease due to samples being cut out from the smaller rock types not used in the analysis.

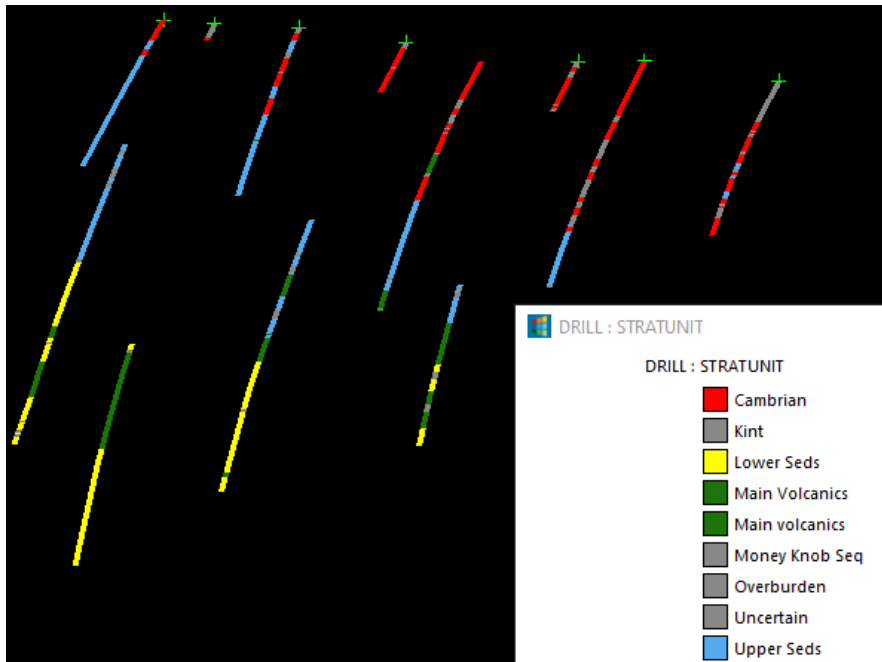


Figure 3: A 2D view example of the drill holes analyzed. The different colors associated with each drill hole represent a different rock type (Red - CAM, Blue - UPS, Green - MVC, and Yellow - LOS). It should be noted that the gray rock types are not utilized in this study.

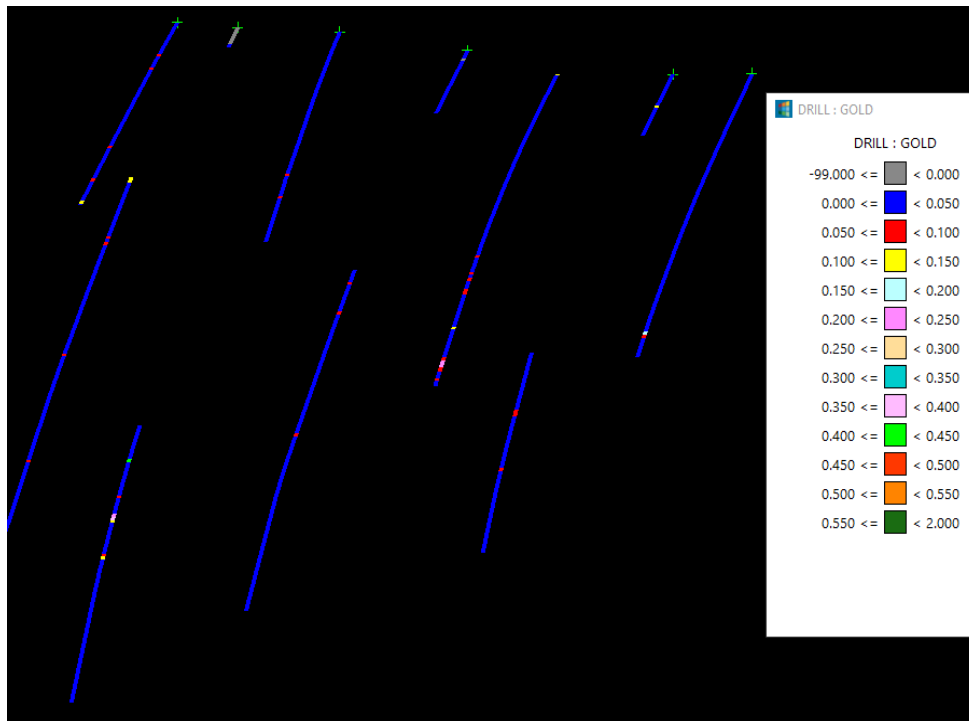


Figure 4: An example of gold grade estimations (g/mt) after compositing through all the four rock types considered.

Table 3: General statistics of all the gold grades within all rock types identified from the drill cores.

# of Samples	37,723
Mean	0.012
Std. Deviation	0.031
Variance	0.001
CV	2.720
Max	1.589
Upper Quartile	0.012
Median	0.003
Lower Quartile	0.001
Minimum	0.00

Table 4: General statistics of gold grades associated with the four main rock types used in this study.

Rock Type	# of Samples	Mean	Std. Dev.	Var.	CV	Max	Upper Quart.	Med.	Lower Quart.	Min.
CAM	8,046	0.007	0.037	0.001	5.134	1.412	0.003	0.001	0	0
UPS	10,228	0.011	0.032	0.001	2.937	0.709	0.01	0.003	0.001	0
MVC	8,463	0.02	0.031	0.001	1.563	0.997	0.023	0.013	0.005	0
LOS	7,155	0.009	0.027	0.001	3.025	1.589	0.009	0.003	0.001	0

3.2 - Geological Modeling

Using the data gathered from the exploration drilling, a solid of each main rock type was created to ensure the best visualization of the subsurface. It should be noted that in the creation of the solid, experts' knowledge was taken for preparing them. As shown in Figure 5, the blue rock type (UPS) is the most spread out throughout the subsurface while CAM is most concentrated in a single location. Each rock type varies in thickness

throughout the study area. Since each solid is based on the drill cores, each rock type's solid could only be made where drill cores were extracted. Not all places within the study area could be reached by drilling, hence the gaps present between rock types. Each solid created is valid, closed, and does not have any other discrepancies associated with it. The appended solid, as shown in Figure 6, demonstrates when the rock types are combined, forming one orebody. The orebody still shows the full distribution of the rock types in the subsurface and does not exclude any part of a single rock type. Importantly, the appended solid is also valid, closed, with no discrepancies associated with its creation.

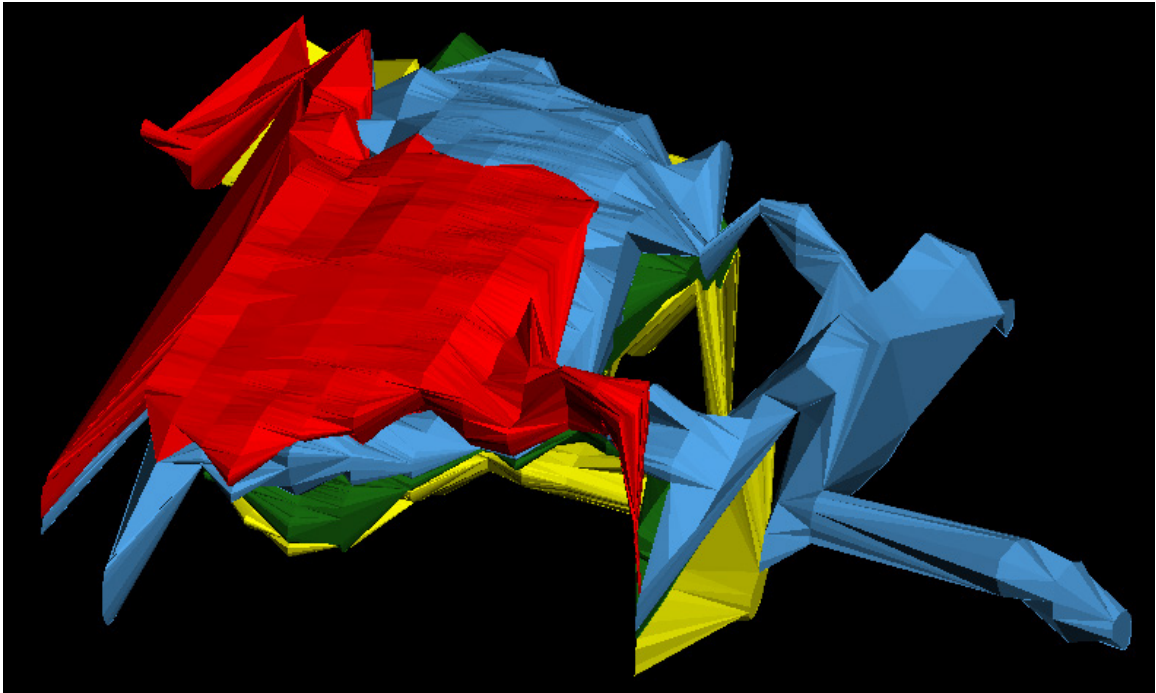


Figure 5: An illustration of the four main rock types in a solid form (Red - CAM, Blue - UPS, Green - MVC, and Yellow - LOS). This shows the layering of each rock type relative to one another, and how each rock type is distributed in the subsurface

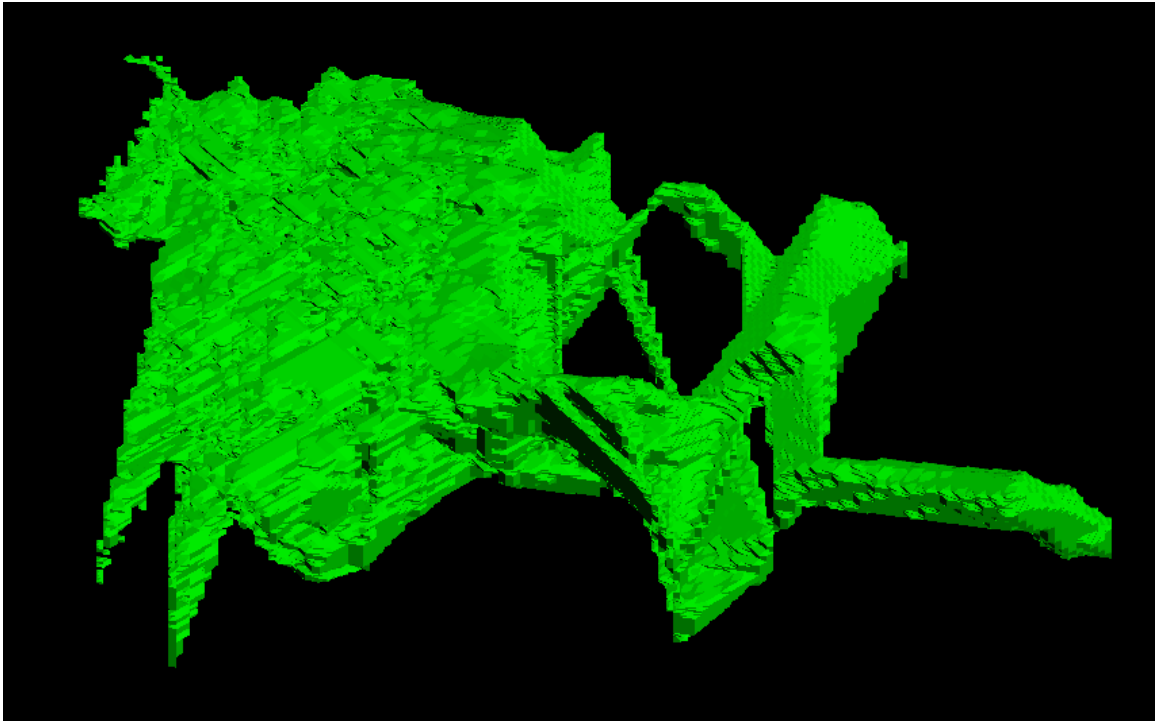


Figure 6: The appended solid of the four main rock types illustrating the complex geology in the study area. This orebody is utilized in grade estimation.

Figure 7 shows the best fitted theoretical variogram with a spherical structure along with its respective parameters, as illustrated in Table 5, with a lag size of 10 and lag tolerance of five. Directional anisotropy was analyzed and found absent in the data. Figure 7 shows the general distribution of gold grades from the OK conducted, with its associated statistics shown in Table 6. The distribution of gold grades is skewed to the left, with little to no data following the right side of the histogram. Figure 8 gives an illustration of the OK gold grade results implemented in a block model with the topographical surface shown, giving a full 2D example of how the gold grades are spread out in the subsurface. There is no pattern with the gold grades or concentration of gold as they are distributed at random within the subsurface.

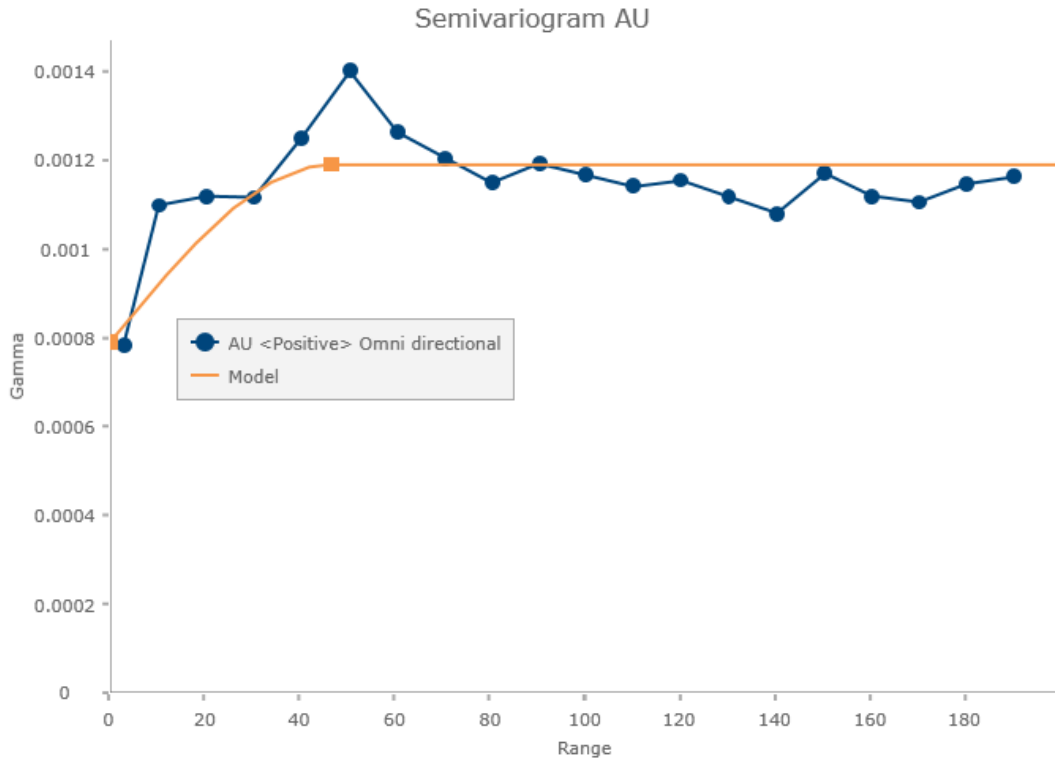


Figure 7: Best fitted, omnidirectional variogram for the gold grades in the OK process.

Table 5: Parameters for the omnidirectional variogram.

Variogram Type	Total Sill	Range	Nugget
Spherical	0.00119	46.349	0.00079

Table 6: General statistics from the histogram of the OK gold grade results found in the orebody.

	Orebody
Total # of Samples	43,442
Mean	0.01
Std. Dev.	0.014
Variance	0
CV	1.357
Max	0.246
Upper Quart.	0.014
Med.	0.006
Lower Quart.	0.002
Min.	0

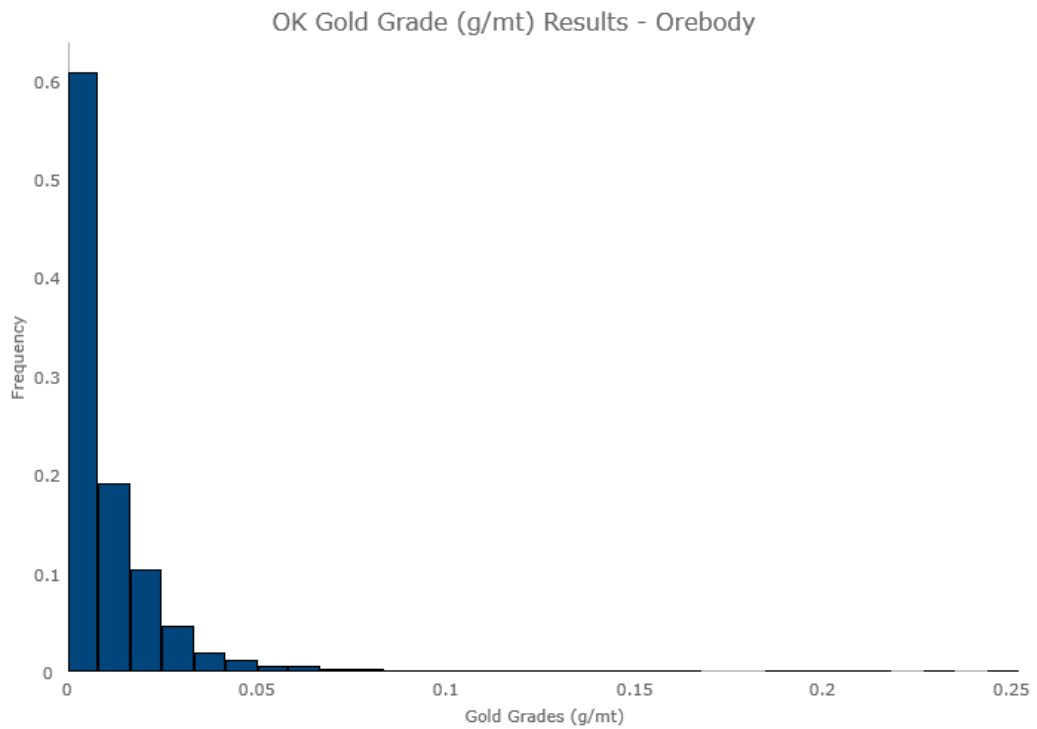


Figure 7: Histogram of OK results within the orebody.

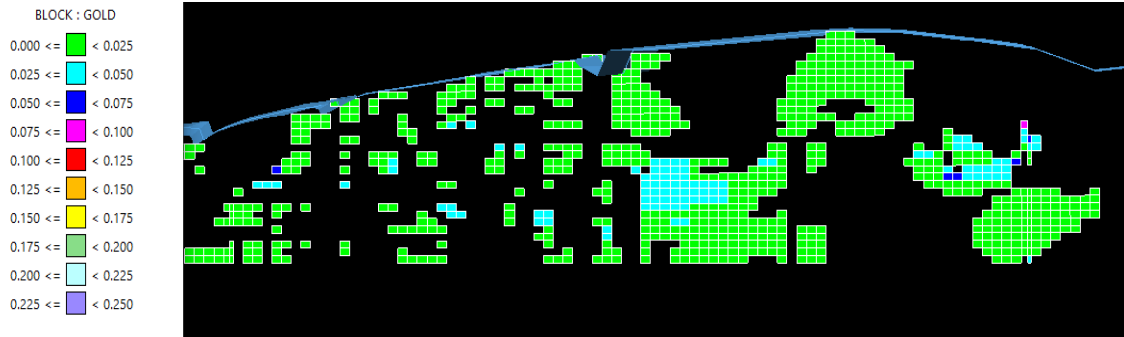


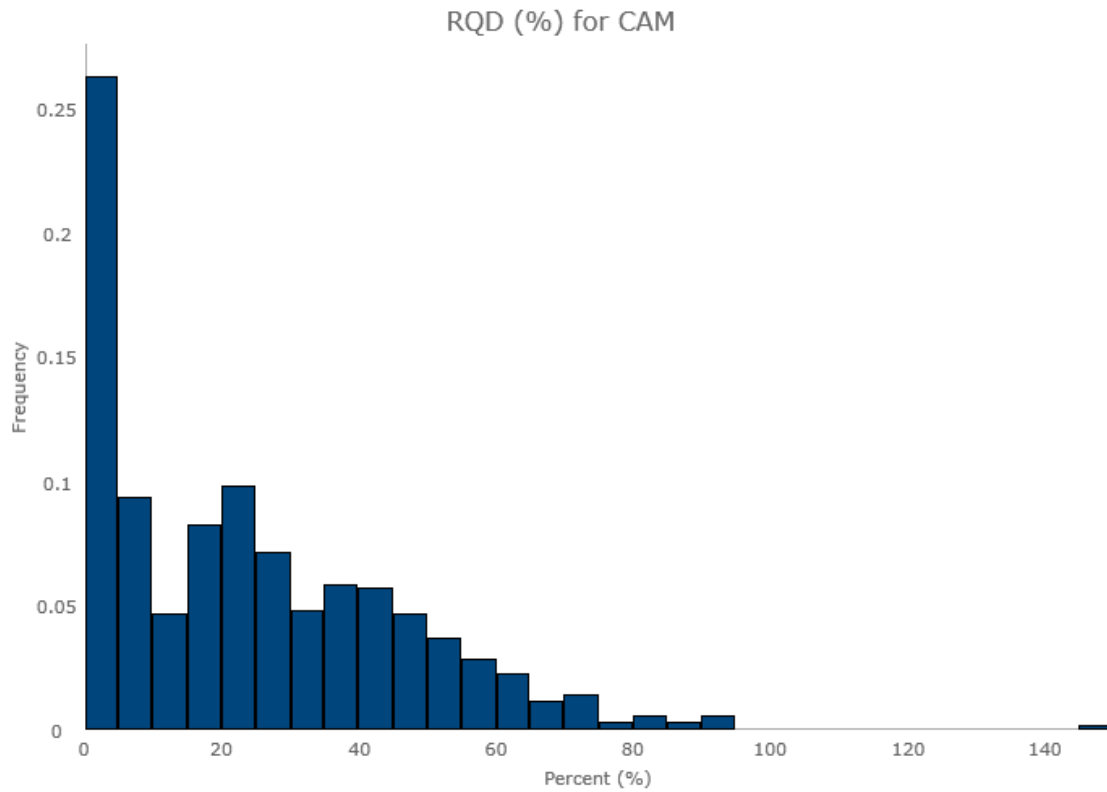
Figure 8: Gold grade distribution shown in a 2D view, with topographical surface applied (blue) to illustrate the gold deposits extent in the subsurface.

3.3 - RQD Percentages of Each Rock Type

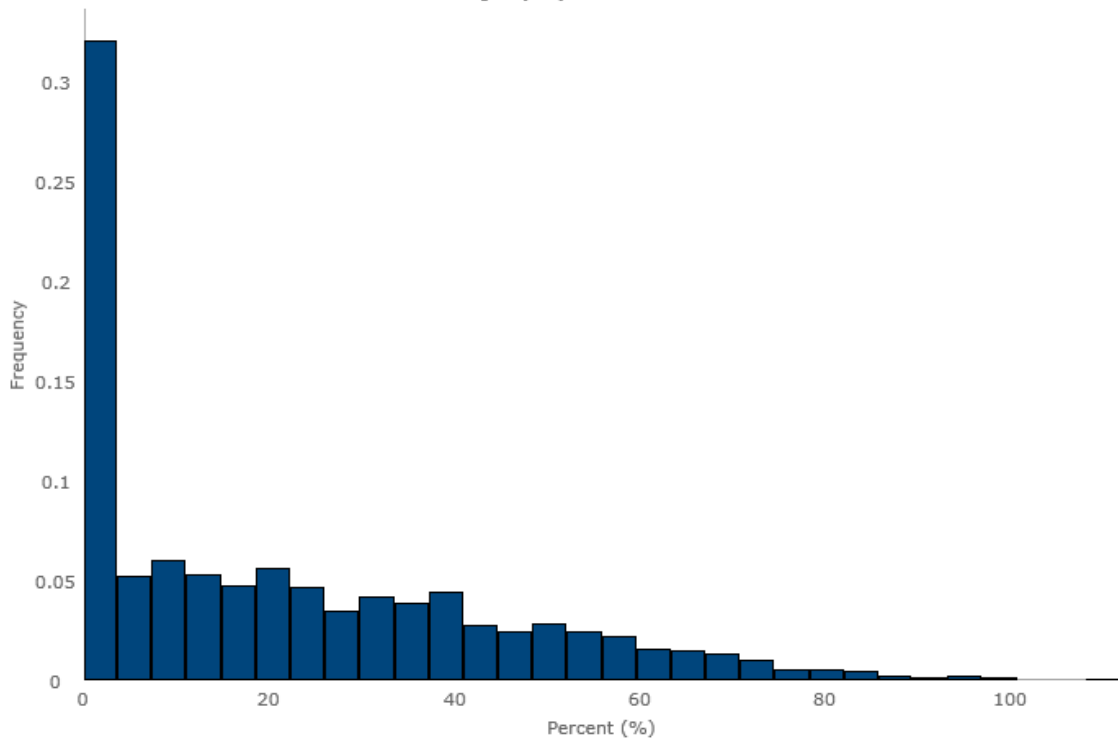
Figure 9 illustrates the range of RQD values recorded for each rock type while Table 7 shows the statistical properties for each rock type. The rock types distributions are all skewed to the left, with very few values to the right of the distribution. The MVC histogram shows more values spread through the histogram but ultimately stays skewed to the left. However, it's clear that the RQD for the four rock types are poor, which is due to the environment and faulting that occurred here. The strongest rock type present is MVC with a mean value of 36.951 while the weakest rock type seems to be the LOS with a mean value of 15.628. The difference of strength values could be due to how much deformation occurred with each rock type along with the composition of each. Alongside that, this difference is to be expected as igneous rocks are generally stronger than sedimentary rocks. Variances are high within Table 7 due to the scarcity of the data, but the general statistics are still applicable. An anova test was conducted on the RQD data to show the statistical significance (Table 8). The F-value and p-value results from anova test reject the null hypothesis, meaning the means of RQD from different rock type are not the same. Thus, the RQD data from each rock type was modeled separately.

Table 7: Statistical properties for each rock type regarding RQD values.

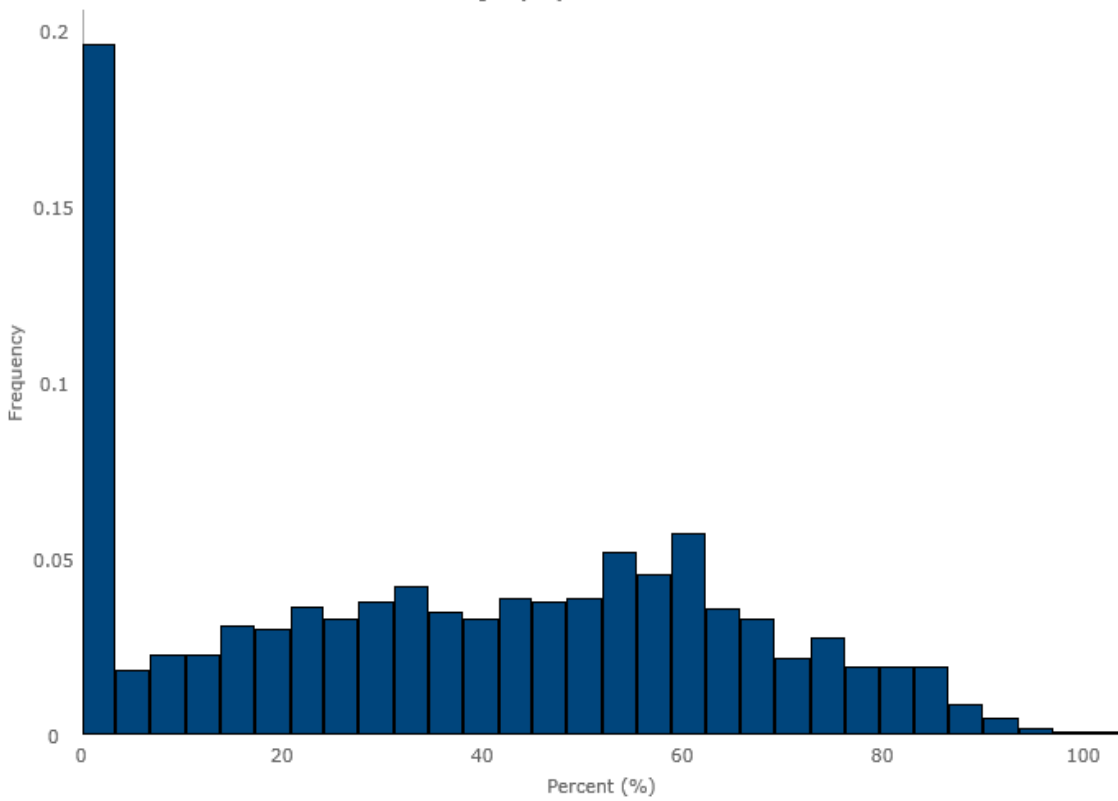
Rock Type	# of Samples	Mean RQD %	Std. Dev.	Var.	CV	Max	Upper Quart.	Med.	Lower Quart.	Min.
CAM	702	23.71	21.84	476.97	0.92	147.84	38.03	20.24	3.68	0
UPS	3030	21.78	22.31	497.9	1.03	109.73	37	16	0	0
MVC	1739	36.95	26.77	716.61	0.72	101	58.66	37.8	12	0
LOS	1666	15.63	19.57	383.16	1.25	128	26	8	0	0



RQD (%) for UPS



RQD (%) for MVC



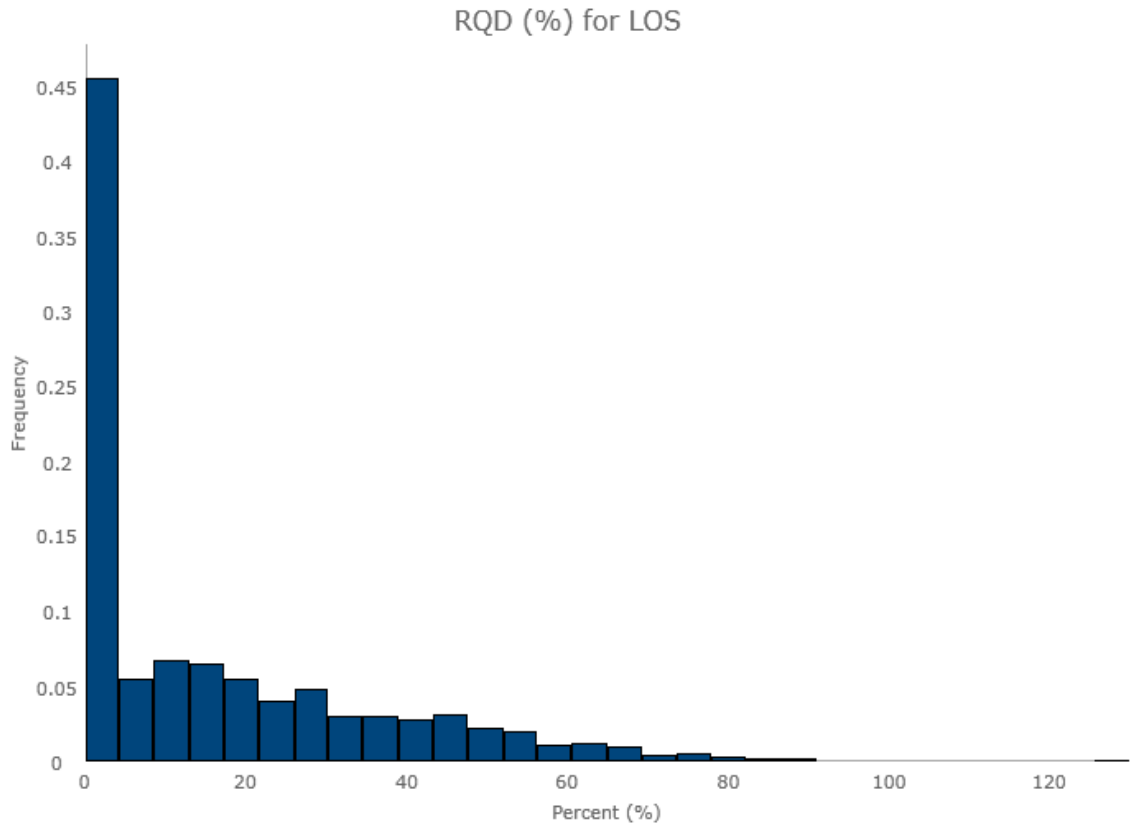


Figure 9: Histograms of RQD percentages for each rock type.

Table 8: Anova test results illustrating that the population means are not equal. *** signifies the data is less than 0.001.

	Df	Sum Sq	Mean Sq	F Value	Pr (>F)
Geocode	3	423155	141052	269.9	<2e-16***
Residuals	7133	3728004	523		

3.4 - Slope Stability

Based on the histograms for each rock type, 1000 random RQD values were assessed using Monte Carlo sampling for a stochastic analysis. Using Table 2, conversions were made with each RQD sample to obtain a cohesion value, angle of internal friction, and unit weight. Table 9 shows the mean values of 1000 random samples of these properties for all four rock types. From Table 9, most of the samples are in the very poor to poor quality range which yields a low cohesion and internal friction angle. The values for cohesion and internal friction for all rock types are relative to one another besides the MVC value. As mentioned earlier, due to its volcanic nature and igneous composition, it is expected that this rock type should yield a higher strength compared to the others.

Table 9: Data used for material properties of the slope stability analysis.

Rock Type	RQD (%) based off K samples via. histogram	Variance	Unit Weight (kN/m ³)	Mean Cohesion (kPa) and (Std. Deviation)	Mean Friction Angle (degree) and (Std. Deviation)	Histogram Type
CAM	23.713	476.968	20	150 (11059.62)	15 (10.83)	Log-Normal
UPS	21.775	497.902	20	150 (2221.38)	15 (7.09)	Log-Normal
MVC	36.951	716.612	20	750 (2193.59)	20 (6.82)	Log-Normal
LOS	15.628	383.157	20	150 (2237.74)	15 (7.19)	Log-Normal

A single slope with a catch bench was inputted to get an idea of how different slope angles affected the stability of the overall slope. The slope angles' range was selected based off Kring & Chatterjee's (2020) work, since the same data set is used here. The slope angles evaluated were picked at random between the range given. The minimum angle considered is 37° and maximum slope angle is 56°. A total number of nine slope angles were evaluated using Monte Carlo simulation. The results produce a histogram that shows the FoS values generated. However, for simplistic purposes, only the 56° histogram is being demonstrated (Figure 12). Each histogram shows the range of FoS values that are evaluated through the 1000 simulations. It utilized a log-normal distribution with it being heavily skewed to the left. Based on the simulations, mean factor of safety, variance of factor of safety, and probability of failure were calculated for three different factors of safety, and are presented in Table 10.

The results demonstrated that angles 37 through 50 showed no probability of failure while angles 51 through 56 indicated probability of failures as the FoS increased. This is expected as lower slope angles yield a higher FoS and high reliability due to the load being less on the slope. Once a load reaches the maximum stress on a slope, probability of failure increases. In this case, its demonstrated that after the slope is increased past 50 degrees, the slope begins to experience higher levels of stress which increases the probability of failure. From then on, the steeper the slope angle assessed, the higher the probability of failure was within all three FoS ranges. Some discrepancies arise in the mean and variance FoS calculations due to having to filter out negative values that were generated during the slope stability analysis, hence giving lower values than the rest of the slope angles analyzed. The three different FoS were used to demonstrate a conservative vs. risk-taking approach, depending on the mining operation's needs and based on industry standards. Figure 11 shows an example of the slope design used for the slope stability analysis with the four rock types assigned to it. Thicknesses of each rock type were estimated based on a 2D cross sectional view of each rock type in the block model as shown in Figure 10.

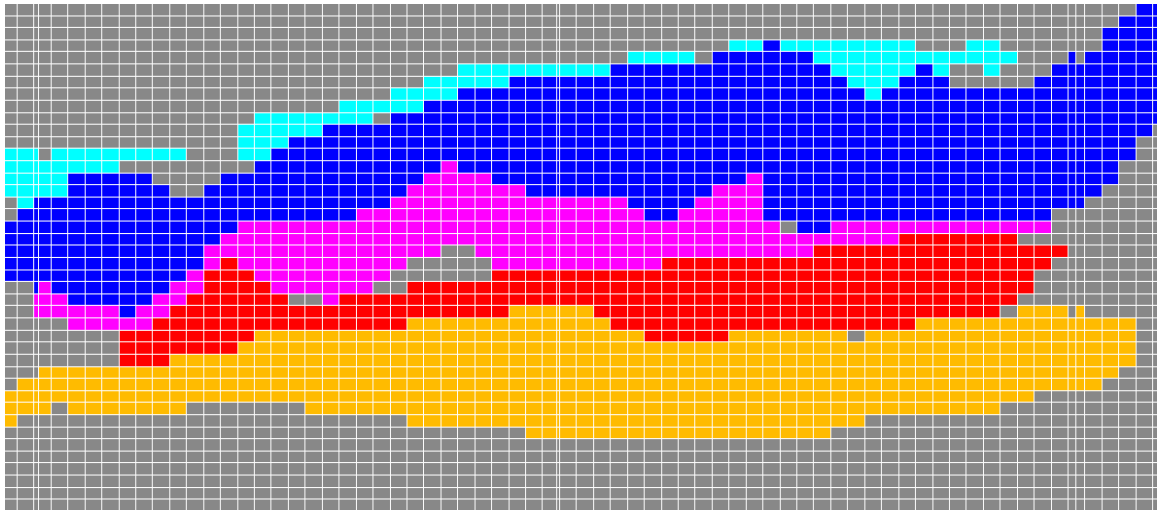


Figure 10: The different rock types illustrated in the block model and used for thickness estimation in Slide2. Blue - CAM, Pink - UPS, Red - MVC, and Yellow - LOS. The teal at the top encompasses the rocks that were not used in this analysis.

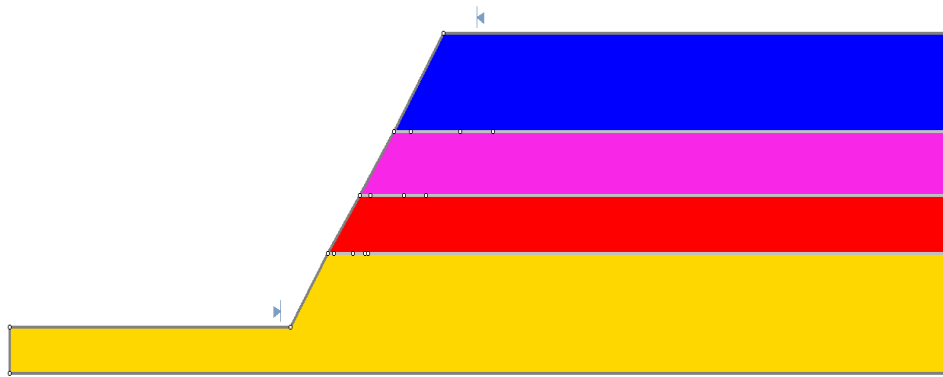


Figure 11: An example of the slope design used. This picture specifically uses a 56° slope angle to be analyzed for slope stability. The layers top down go CAM, UPS, MVC, LOS. Each rock type is assigned with its respective simulated strength parameters.

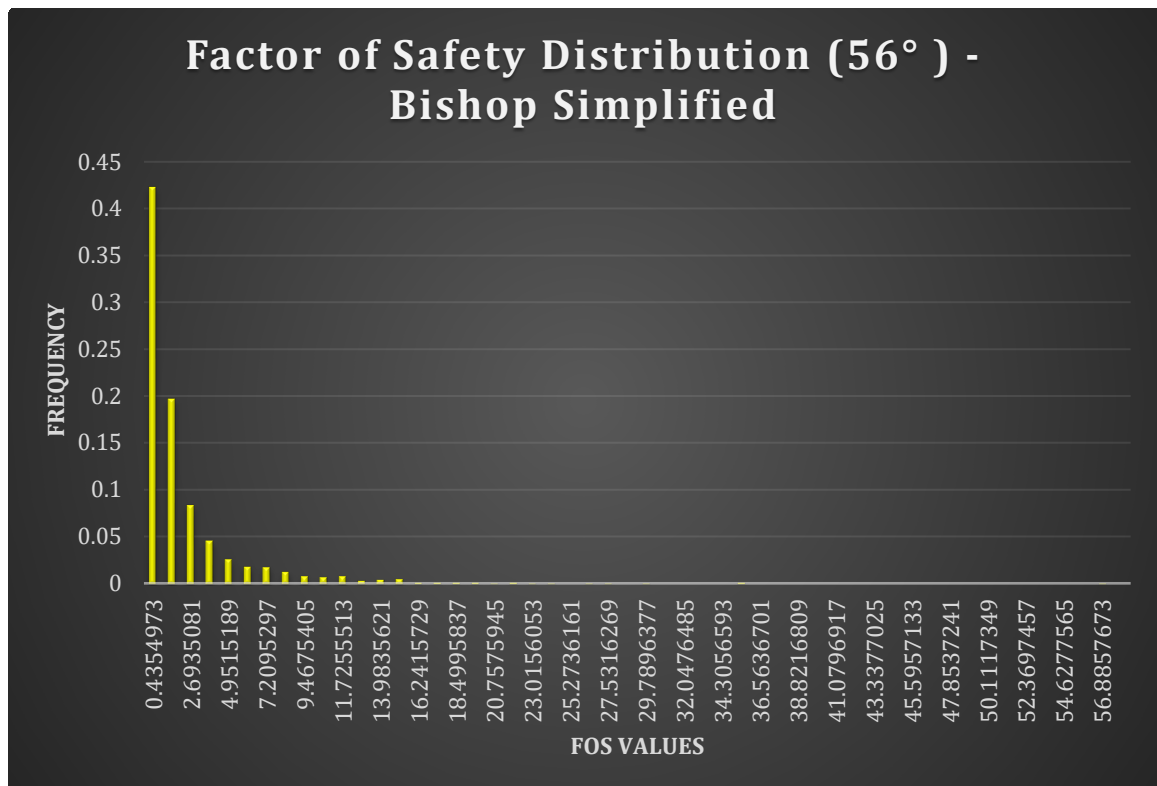


Figure 12: A histogram illustrating the FoS log-normal distribution from the 56° slope stability analysis.

Table 10: Probability of failure percentages for each slope angle evaluated, with respect to the given FoS utilized.

Slope Angle	Mean FoS	Variance of FoS	Probability of Failure (%) with FoS 1.0	Probability of Failure (%) with FoS 1.25	Probability of Failure (%) with FoS 1.5
37	27.328	672.695	0	0	0
39	26.169	593.035	0	0	0
42	24.650	489.066	0	0	0
48	12.613	48.732	0	0	0
49	11.433	30.564	0	0	0
50	11.296	29.430	0	0	0
51	9.593	772.504	31.3	37.7	43
54	2.340	12.857	47	53	59
56	2.612	19.271	48	54	60

3.5 - Pit Optimization

Pit optimization was conducted with, at the time of writing this, a gold price of \$1852.0 per ounce (oz av). Multiple pits were generated with each slope angle used and Figure 13 shows an example of two of the nine pits generated. Table 11 illustrates the different cash flows each angle yields, while incorporating the probability of failure values from each FoS evaluated from the slope stability analysis. This demonstrates that the lower slope angles yield less cash flow than the steeper slope angles used. The range of the cash flow varies greatly as there is a ~701-million-dollar (US dollar) difference between the lowest slope angle evaluated (37°) and highest slope angle evaluated (56°). The difference of one degree as shown with the jump from 50° to 51° illustrates how critical a slope angle is for an open pit mining operation as the profit generated increases roughly by ~40 million dollars (US dollar). However, a higher probability of failure resides in the steeper slope angles which is to be expected. Due to the constantly changing price of gold, these prices may increase or decrease which could influence a mining operations decision on which angle yields most profitable. This decision will ultimately be decided within the constraints the FoS probability of failure produces, as this ensures a safe mining operation will be in

place. Figure 14 shows a graphical illustration of how slope angles influence the profit and probability of failure. Based on Figure 14, where the profit generated and probability of failure intersect, a threshold slope angle can be determined. This angle, 51.5° , is the maximum slope angle that could be used since exceeding slope angles illustrate the probability of failure outweighs the profit generated. With this knowledge, recommendations could be made. If one were to choose a conservative approach, using a FoS of 1.25, and ensure there is theoretically zero chance of failure while still generating the most profit, a slope angle of 50° would be the optimal choice. In contrast, if one decides to do a risk-taking approach utilizing the same FoS, the maximum slope angle that could be used is the threshold value, 51.5° , as the probability of failure outweighs the profit generated for steeper slope angles.

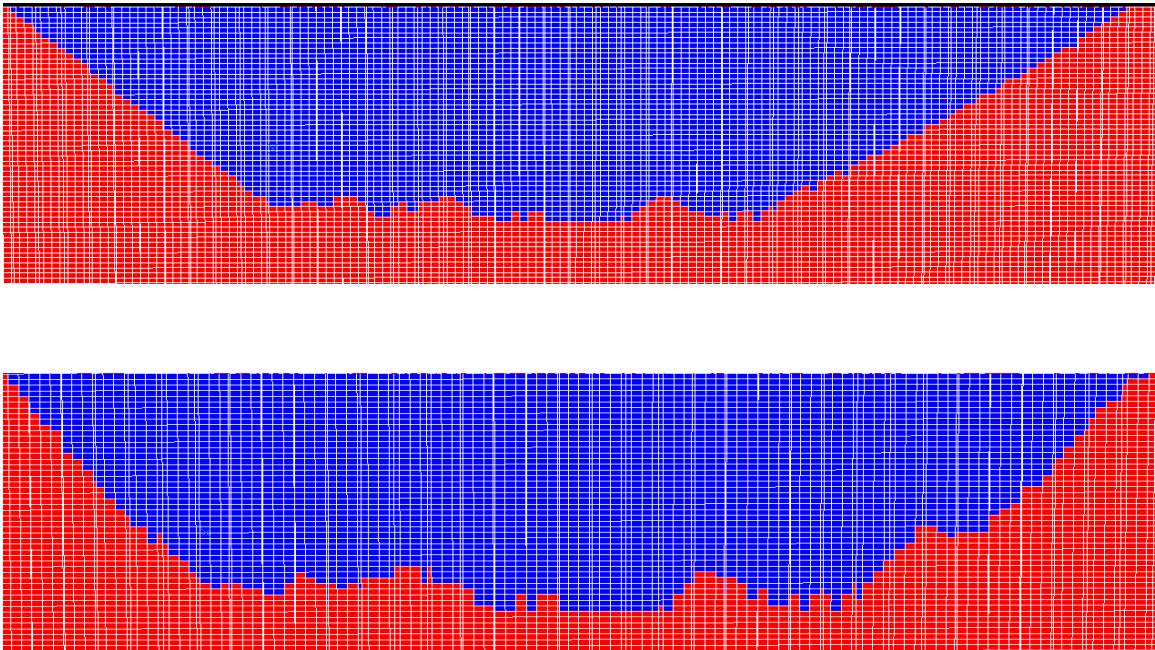


Figure 13: Illustration of the ultimate pit generated. These were generated for pit optimization. The top picture is a slope angle of 37° , while the bottom picture uses a slope angle of 56° .

Table 11: Each slope angle evaluated with its probability of failure based on a given FoS, along with its economic value if used for the open pit mine.

Slope Angle	Probability of Failure (%) with FoS 1.0	Probability of Failure (%) with FoS 1.25	Probability of Failure (%) with FoS 1.5	Economic Value (\$US Billions)
37	0	0	0	2.234
39	0	0	0	2.326
42	0	0	0	2.462
48	0	0	0	2.684
49	0	0	0	2.721
50	0	0	0	2.741
51	31.3	37.7	43	2.787
54	47	53	59	2.895
56	48	54	60	2.935

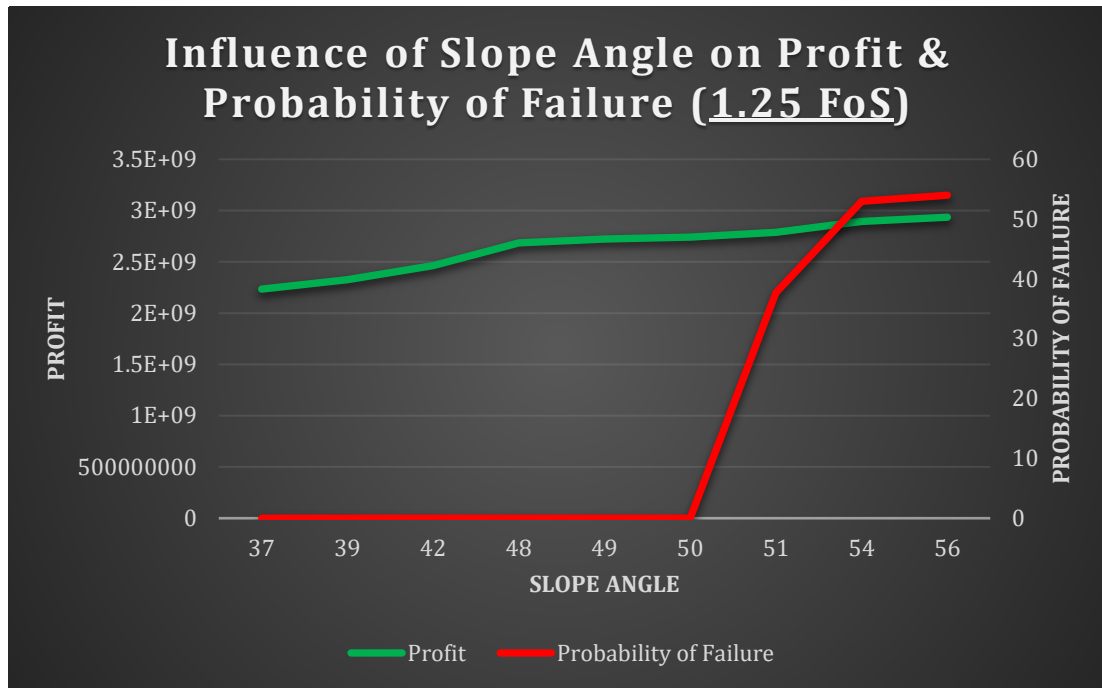


Figure 14: An illustration of how different slope angles influence the profit and probability of failure using a FoS value of 1.25.

4. Conclusion

This research encompasses geomechanical uncertainty with ultimate pit optimization. The gold grade data from exploration drilling are estimated with OK to have an estimation of the total gold deposit in the subsurface. Since there was limited RQD data given from the initial exploration drilling, a slope stability analysis was conducted using nine slope angles, utilizing the same data set as Kring & Chatterjee (2020). Each slope angle yields different probabilities of slope failure, given the different rock strength parameters. Once the slope angles were assessed, pit optimization was conducted to see the economic value (cash flow) each angle yielded with the gold grades (Table 11). The higher slope angles yielded a greater profit while the lower slope angles did not generate as much cash flow. A threshold value of 51.5° was determined based on Figure 14 and should not be exceeded due to the probability of failure outweighing the profit generated from steeper slope angles. The steeper the slope angle used, the higher the chance of failure is for the slope.

4.1 Limitations and Further Studies

It is very important to note that stability analysis results are dependent on the location of the pit slope. A slope stability analysis would need to be conducted in every location of the pit to ensure a stable slope angle is utilized. This analysis uses a simplified model for slope stability analysis to showcase the impact of geomechanical uncertainty on open pit mine planning. Therefore, several assumptions were made to conduct this research. For example, no rock fracture and freeze-thaw mechanism from the frigid Alaska weather were not considered. Moreover, only one single mechanism of slope failure was considered. Further research should look at these assumptions further to provide a more reliable model and results overall. However, the scope of this research illustrates that incorporating geomechanical uncertainty is possible in open pit optimization, using the methods presented in this paper.

5. References

- Abbaszadeh, M., Shahriar, K., Sharifzadeh, M., & Heydari, M. (2011). Uncertainty and reliability analysis applied to slope stability: a case study from Sungun copper mine. *Geotechnical and Geological Engineering*, 29, 581-596.
- Abdulai, M., & Sharifzadeh, M. (2021). Probability methods for stability design of open pit rock slopes: an overview. *Geosciences*, 11(8), 319.
- Abdulai, M., & Sharifzadeh, M. (2019). Uncertainty and reliability analysis of open pit rock slopes: a critical review of methods of analysis. *Geotechnical and Geological Engineering*, 37, 1223-1247.
- Baek, J., Choi, Y., & Park, H. S. (2016). Uncertainty representation method for open pit optimization results due to variation in mineral prices. *Minerals*, 6(1), 17.
- Benndorf, J., & Dimitrakopoulos, R. (2013). Stochastic long-term production scheduling of iron ore deposits: Integrating joint multi-element geological uncertainty. *Journal of Mining Science*, 49(1), 68-81.
- Chatterjee, S., Sethi, M. R., & Asad, M. W. A. (2016). Production phase and ultimate pit limit design under commodity price uncertainty. *European Journal of Operational Research*, 248(2), 658-667.
- Curran, J. H., & Hammah, R. E. (2006). Seven lessons of geomechanics software development. In *Proceedings of the 41st US Symposium on Rock Mechanics (USRMS)*, American Rock Mechanics Association, Minneapolis, MN.
- Dagdelen, K. (2001, June). Open pit optimization-strategies for improving economics of mining projects through mine planning. In *17th International Mining Congress and Exhibition of Turkey* (Vol. 117, p. 121).
- Deere, D. U., & Deere, D. W. (1988). The rock quality designation (RQD) index in practice. In *Symposium on Rock Classification Systems for Engineering Purposes, 1987*, Cincinnati, Ohio, USA.
- Dimitrakopoulos, R., & Ramazan, S. (2004). Uncertainty based production scheduling in open pit mining. *SME transactions*, 316.

- Dunn, M. J. (2019, April). Quantifying uncertainty in mining geomechanics design. In *MGR 2019: Proceedings of the First International Conference on Mining Geomechanical Risk* (pp. 391-402). Australian Centre for Geomechanics.
- Ecker, M. D., & Gelfand, A. E. (1999). Bayesian modeling and inference for geometrically anisotropic spatial data. *Mathematical Geology*, *31*, 67-83.
- Hack, R., Orlic, B., Ozmutlu, S., Zhu, S., & Rengers, N. (2006). Three and more dimensional modelling in geo-engineering. *Bulletin of Engineering Geology and the Environment*, *65*, 143-153.
- Hlajoane, S. A. (2020). *Joint Simulation of Continuous and Categorical Variables for Mineral Resource Modeling and Recoverable Reserves Calculation* (Doctoral dissertation, Michigan Technological University).
- Hochbaum, D. S. (2001). A new—old algorithm for minimum-cut and maximum-flow in closure graphs. *Networks: An International Journal*, *37*(4), 171-193.
- Huang, Y. H. (2014, February). Slope stability analysis by the limit equilibrium method: Fundamentals and methods. American Society of Civil Engineers.
- Hustrulid, W. A., Kuchta, M., & Martin, R. K. (2013). *Open pit mine planning and design, two volume set & CD-ROM pack*. CRC Press.
- Kapageridis, I., Apostolikas, A., Pappas, S., & Zevgolis, I. (2013). Use of mine planning software for the evaluation of resources and reserves of a sedimentary nickel deposit. *Bulletin of the Geological Society of Greece*, *47*(4), 1980-1989.
- Kring, K., & Chatterjee, S. (2020). Uncertainty quantification of structural and geotechnical parameter by geostatistical simulations applied to a stability analysis case study with limited exploration data. *International Journal of Rock Mechanics and Mining Sciences*, *125*, 104157.
- Liu, S. Y., Shao, L. T., & Li, H. J. (2015). Slope stability analysis using the limit equilibrium method and two finite element methods. *Computers and Geotechnics*, *63*, 291-298.
- Lu, Y., Tan, Y., & Li, X. (2018). Stability analyses on slopes of clay-rock mixtures using discrete element method. *Engineering Geology*, *244*, 116-124.

- Menabde, M., Froyland, G., Stone, P., & Yeates, G. A. (2018). Mining schedule optimisation for conditionally simulated orebodies. *Advances in applied strategic mine planning*, 91-100.
- Mitma, C. A. O. (2020). *Slope Stability Analysis of Open Pit Mines under Geomechanical Uncertainty* (Doctoral dissertation, McGill University (Canada)).hu
- Ning, Y. J., An, X. M., & Ma, G. W. (2011). Footwall slope stability analysis with the numerical manifold method. *International Journal of Rock Mechanics and Mining Sciences*, 48(6), 964-975.
- Obregon, C., & Mitri, H. (2019). Probabilistic approach for open pit bench slope stability analysis—A mine case study. *International Journal of Mining Science and Technology*, 29(4), 629-640.
- Paithankar, A., Chatterjee, S., & Goodfellow, R. (2021). Open-pit mining complex optimization under uncertainty with integrated cut-off grade based destination policies. *Resources Policy*, 70, 101875.
- Phoon, Kok-Kwang, Zi-Jun Cao, Jian Ji, Yat Fai Leung, Shadi Najjar, Takayuki Shuku, Chong Tang, Zhen-Yu Yin, Yoshida Ikumasa, and Jianye Ching. "Geotechnical uncertainty, modeling, and decision making." *Soils and Foundations* 62, no. 5 (2022): 101189.
- Read, J., & Stacey, P. (2009). Guidelines for open pit slope design.
- Rocscience Slide2 [Computer software]. (2022). Retrieved from <https://www.rocscience.com/>
- Soren, K., Budi, G., & Sen, P. (2014). Stability analysis of open pit slope by finite difference method. *Int. J. Res. Eng. Technol*, 3(5), 326-334.
- Sunday, C. A., & Deutsch, C. V. (2020). Choosing the Discretization Level for Block Property Estimation. *Geostatistics Lessons*.
- Wackernagel, H. (2003). *Multivariate geostatistics: an introduction with applications*. Springer Science & Business Media.
- West, T. R., & Shakoor, A. (2018). *Geology applied to engineering*. Waveland Press.

Zebarjadi Dana, H., Khaloo Kakaie, R., Rafiee, R., & Yarahmadi Bafghi, A. R. (2018). Effects of geometrical and geomechanical properties on slope stability of open-pit mines using 2D and 3D finite difference methods. *Journal of mining and Environment*, 9(4), 941-957.